3. EXPERIMENTAL

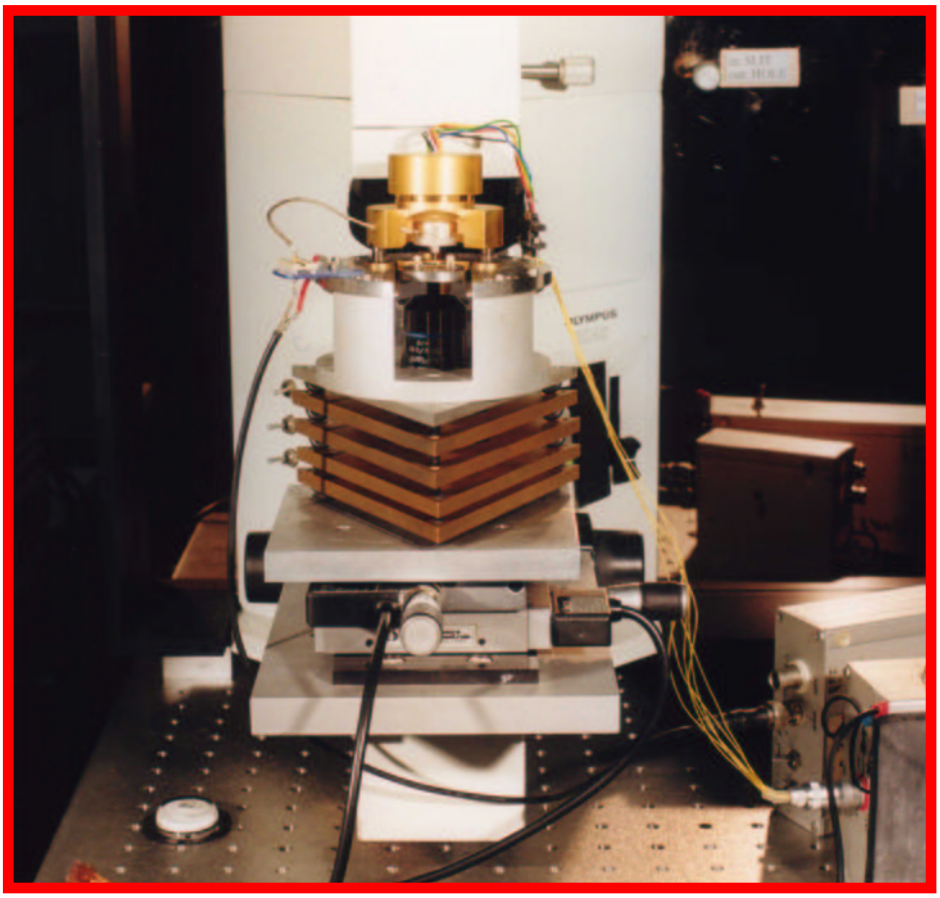

3

3.1 The set-up

Our aim is to evaluate the influence of the external electromagnetic field localized at the tip apex; for that purpose, Raman (vibrational) spectra are recorded from molecules adsorbed at the opposing metal surfaces and located directly underneath the tunneling tip.

The basic need is then to have the tip illuminated by a monochromatic light source. Stability of the whole system is crucial: the laser spot must be fixed with respect to the tip position. A common and effective solution to suppress most of the vibrations of mechanical origin is to have the STM (apart from the electronics) suspended with elastic ropes. Such a simple arrangement could not be readily adopted in our case due to the additional presence of the laser and spectrograph. We opted for a combination of passive (pneumatics and elastomers) and active damping elements for the whole system. A vibration isolation system from Halcyionics (Mod 2M) isolates against vertical and horizontal displacements in the frequency range between 2 and 10 Hz. Marble slabs are used at the bottom level to increase the overall weight and stability and to shift the vibrational frequency of the set-up to lower values.

The vibrationally isolated Raman microscope, sitting on an optical table, acts as a rigid support for the STM platform and all the elements below it (see Fig. 3.1). A stack of copper plates separated by viton rings provides further protection against low frequency vibrations. X-Y translational stages controlled by piezo-elements enable the lateral movement of the STM platform with respect to the inverted microscope objective which remains fixed in position. The height of the objective may be still changed at will in order to focus the laser light on the tip.

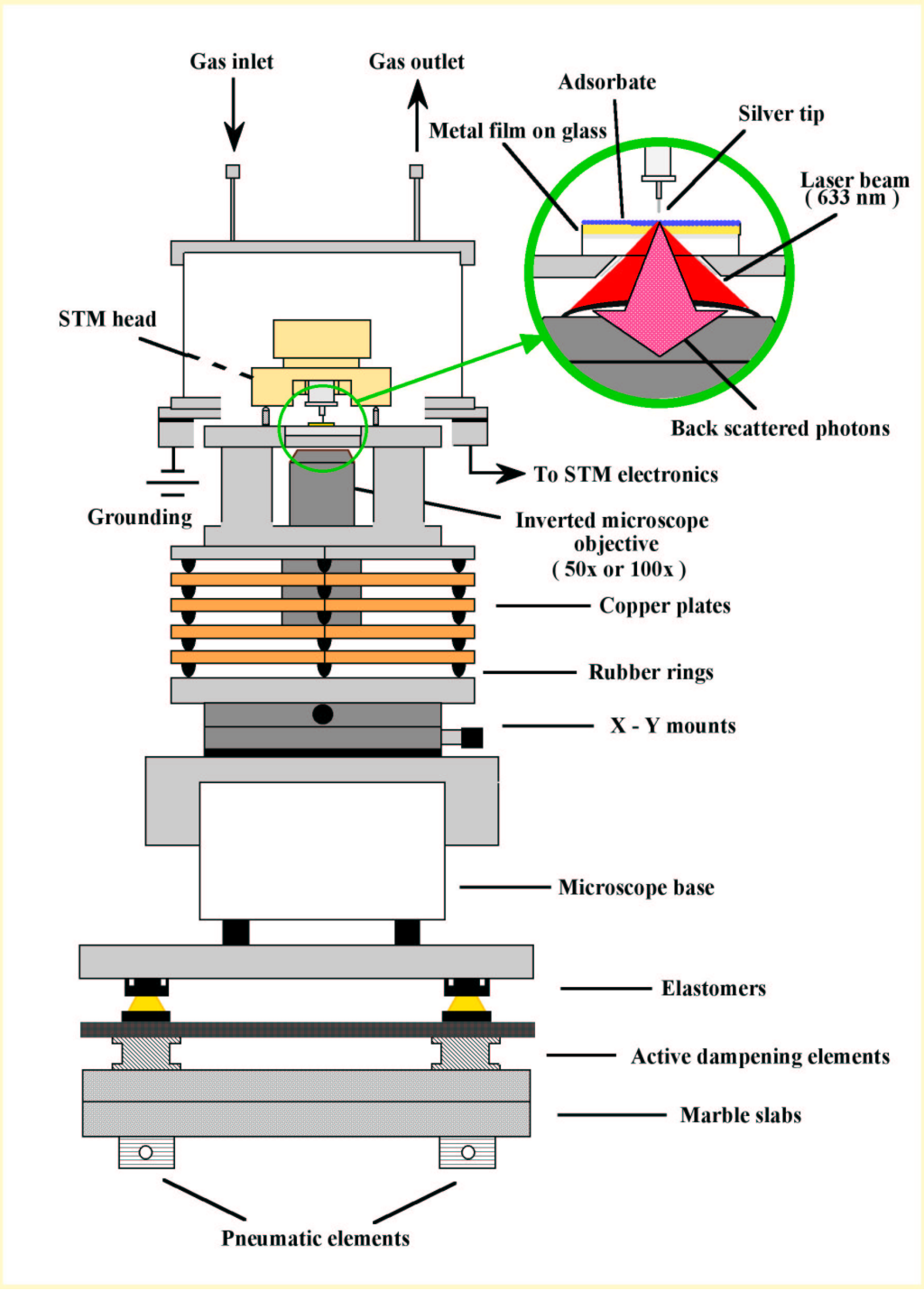

Figure 3.1: Diagram of the coupled Raman STM experimental set up.

With this arrangement, the tip (even when tunneling) may be brought in and outside the laser spot. As can be seen in the inset the tip is placed above a thin metal film covered with the adsorbate and illuminated from below. The inverted objective has two functions. It focusses the laser light from the bottom through the film onto the tip and it collects the Raman photons emitted by the molecules in the back scattering geometry.

The core of the STM head consists of a single lead zirconate titanate piezoelectric tube (EBL 3, Staveley Sensors Inc.). For the electric contacts a silver layer is deposited on the inner and outer walls of the tube. The latter is divided into four sections thus enabling the lateral movement by applying equal and opposite voltages to opposite quadrants. A Kel-F cap mounted onto the bottom of the tube supports the metal tip. The STM platform may hold a sealed glass cage to work in atmospheres other than air. Also, measurements in electrochemical enviroments are possible by mounting a small Kel-F cell pressed onto the film itself.

3.2 The optics

The confocal Raman instrument is a Labram II from Dilor coupled to a BX 40 Olympus microscope. It mainly consists of an Helium-Neon red laser, $\lambda = 632.8$ nm, with nominal power at the output of 10 mW and roughly 2 mW at the spot, two switchable gratings with 600 or 1800 lines per mm (resolution 5.4 and 1.8 cm^{-1}, respectively), a nitrogen cooled CCD camera (800x2000 pixels) and the optics.

The laser beam is directed by mirrors through a pinhole to a first kinematic notch filter, it is then directed to the microscope and collimated by the objective. The scattered light follows the same path back to the notch filter, which rejects the undesired Rayleigh contribution. The Raman light passes through this and a second notch filter, a confocal hole and the entrance slit (their size may be defined by the operator) of the spectrograph. It arrives at the grating, which diffracts it towards the CCD (Charge Couple Device) camera detector. The position angle

of the kinematic notch filter with respect to the beam defines the cut off window: low frequency modes (down to 40 cm^{-1}) may also be investigated whilst any laser light is still blocked. In this work three different objectives were used, all from Olympus, two LMPlanFI 100x and 50x with numerical aperture respectively 0.80 and 0.50 and an LMPlanIR 50x, n.a. 0.55, better suited for measurements in the near infrared.

3.3 Film preparation

All films used were prepared by evaporation using a BOC Edwards Auto 306 control unit coupled to an FL 400 evaporating chamber. An ultrasonically cleaned microscope glass slide of dimensions 10 mm by 10 mm or 10 mm by 20 mm was used as a substrate. Before depositing the gold films (99.999 % purity), a 1 nm chromium film (same purity) was usually pre-deposited to improve the film adherence. For the TERS investigations three different kinds of films were tested: *a)* in the inverted microscope approach, smooth films with thicknesses below 12 nm were needed to have sufficient power reaching the upper surface of the film; *b)* thicker films (250 nm), electrochemically roughened were used in the side illumination approach; *c)* again in combination with the inverted microscope set-up, mildy activated thin films.

An extremely Raman active surface can be obtained by a suitable roughening procedure [98], that consists of sequential potential sweep oxidation-reduction cycles (ORC) in 0.1 M KCl applied (in our case) to the thicker films or in general to massive electrodes. The scan rate was set at 200 mV s^{-1} with potential limit –300 mV and 1200 mV *vs* SCE. 20-25 cycles proved to be sufficient and the stability of the surface with respect to its activity in ambient atmosphere was excellent. The roughness consists of a whole range of submicrometer particles and porous structures created by the dissolution of gold layers and their subsequent redeposition. An SEM image of a gold film treated as described is shown in Fig. 3.2a. Such

a roughening procedure could not be applied to the thinner gold films; a mild, still sufficient, activation was then performed by electrochemically depositing a few monolayers of gold from a 10^{-3} M $HAuCl_4$ solution. Using a gold wire as a counterelectrode, 7 mC of current were passed through the cell, corresponding to roughly 5-6 layers, for an area of 1 cm^2. Such an electrochemical deposition is not homogeneous and the surface showed Raman activity (by visual inspection, the surface appears colored in a dark reddish brown colour). An image of such an electrode is shown in Fig. 3.2b. Silver electrodes were also tested for comparative purposes and to record reference spectra. The roughening procedure is similar as for gold: the same solution and scan rate was used but in a different potential window, from –300 mV to 250 mV, usually the electrode was removed after keeping it polarized for few seconds at the cathodic limit.

For the STM light emission experiments the thicker films were preferred. The flatness of the surface was improved by repeatedly performing flame annealing in an hydrogen atmosphere followed by rinsing in distilled water.

For all the electrochemical treatments of the surface an in house built poten-

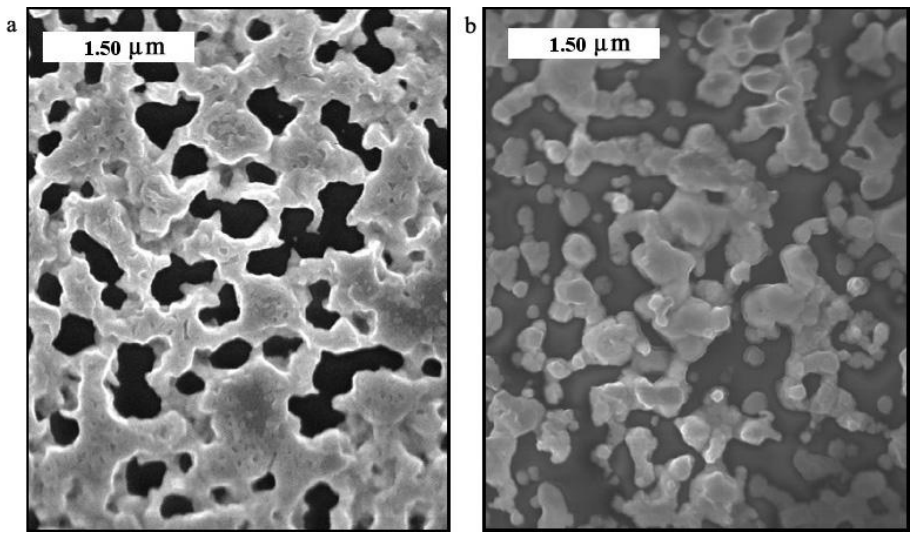

Figure 3.2: SEM images of two differently roughened gold films. On the left, a 250 nm thick film to which oxidation-reduction cycles in 0.1 M KCl were applied; on the right, a thin (12 nm) film onto which gold from a 10^{-3} M $HAuCl_4$ solution was electrochemically deposited.

tiostat, developed and patented by the Institute electronic workshop (FHI-Elab # 2085), was used.

3.4 Tip preparation

Silver and gold tips were used to create the additional (external) Raman enhancement. In chapter two, the way in which the shape and the size of the apex define the field magnitude and extension was discussed. Depending on the excitation wavelength used, tips with curvature radii between 200 nm and 10 nm should give an appreciable enhancement.

Our tips were fabricated by electrochemical dissolution in a proper etching solution [99, 100]. For gold, a concentrated hydrochloric acid solution was used. The overall electrochemical reaction is:

$$\begin{aligned} \mathrm{Au} + 4\ \mathrm{Cl^-} &\longrightarrow \mathrm{AuCl_4^-} + 3\ \mathrm{e^-} \\ \mathrm{H_3O^+} + \mathrm{e^-} &\longrightarrow 1/2\ \mathrm{H_2} + \mathrm{H_2O} \end{aligned}$$

$$3\ \mathrm{H_3O^+} + \mathrm{Au} + 4\ \mathrm{Cl^-} \longrightarrow 3/2\ \mathrm{H_2} + \mathrm{AuCl_4^-} + 3\ \mathrm{H_2O}$$

A small electrochemical cell was used to etch the wire, as depicted in Fig. 3.3. The counter electrode was a small gold ring (diameter of the ring 1 cm) surrounding the wire (diameter 0.25 mm). A constant voltage of 3.0 V was applied to the cell. When the wire was partially immersed into the electrolyte, the etching of the metal proceeded as a necking in around the region closer to the counterelectrode but material was also removed from the lower part of the wire. A small camera with a suitable high magnification was mounted close to the cell permitting to monitor the dissolution process. It can be clearly seen how subsequent layers of materials are stripped from the sides, resulting in a continuous downward flow of material. The etching was stopped manually when the lower end finally dropped.

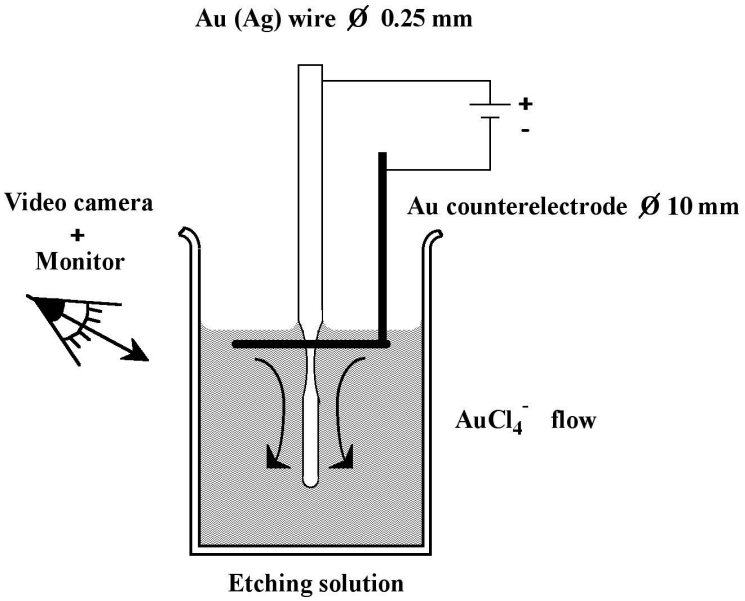

Figure 3.3: Diagram of the electrochemical cell used for etching metal tips.

This occurs when the weight of the remaining part overcomes the cohesional forces inside the polycrystalline thin neck. A blunt tip was obtained if the wire broke too early, an example may be seen in Fig 3.5c. For this reason, it was more convenient to work with the wire partially immersed: as mentioned before, when the circuit was closed, the wire thinned continuously and the final break took place later, leading to a smaller tip radius. It was also found useful to switch from a continuous etching to a pulsed regime ($\tau < 1s$) when the wire was close to the detachment and wait for the process to settle down before allowing further removal of material with the next pulse.

The same procedure was used for etching silver tips: the electrolyte consisted of a perchloric acid, ethanol and water solution (Streuers Chemicals). At the beginning of the etching process, the voltage was 1.8 V and was lowered to 1.4 V when pulses were applied. On the next pages a small gallery of silver and gold tips is shown. It can be seen that very sharp tips with radii in the range between 50 and 100 nm have been obtained; in this range real control of the final radius cannot be achieved by electrochemical methods alone: a single crystallite is usually found at the bottom and its size gives (approximately) the curvature radius of the tip.

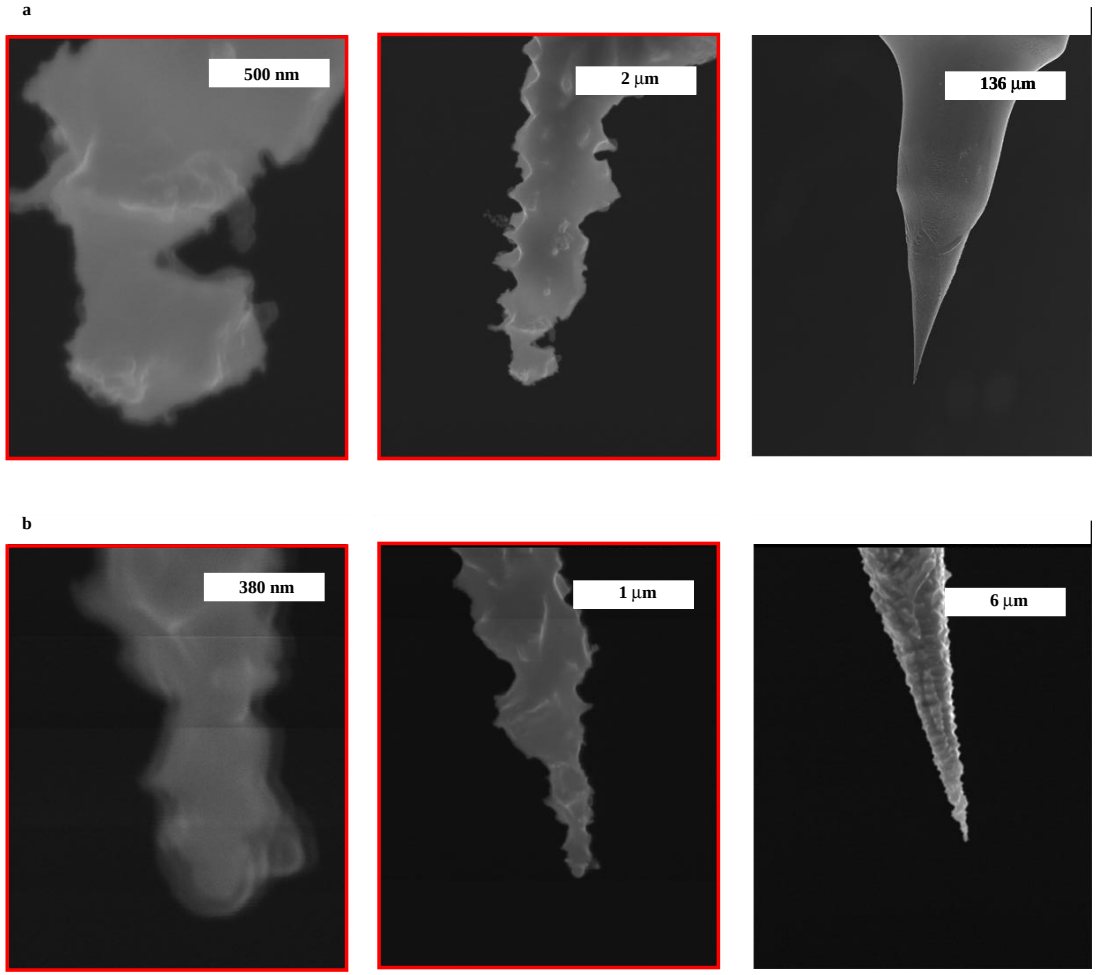

Figure 3.4: Micrographs of electrochemically etched gold tips. A carbon layer contaminated the apex of tip *b* during the adjusting of the gun alignment for recording high resolution SEM images. The etchant was concentrated hydrochloric acid. A scheme of the electrochemical cell used for the etching is shown in Fig. 3.3.

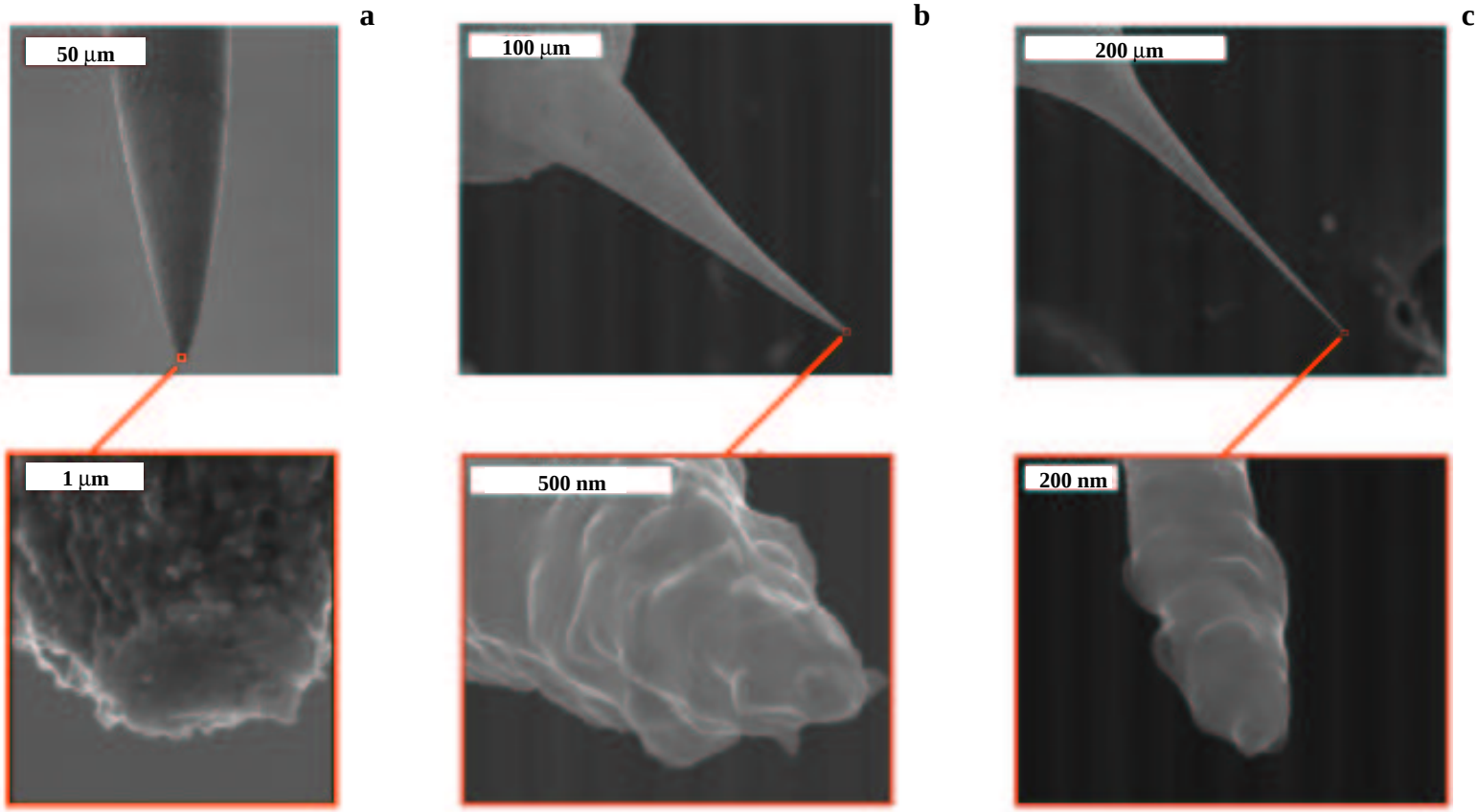

Figure 3.5: Micrographs of electrochemically etched silver tips. The broad and flat apex of tip *a* is not due to a crash during the tunneling but rather to the abrupt detachment of the lower part of the wire during the etching procedure. The etchant was a perchloric acid, ethanol and water solution. A scheme of the electrochemical cell used for the etching is shown in Fig. 3.3.

Usually, the SEM images of the tips were taken after the TERS or light emission experiments.

3.5 Chemicals and reagents

The adsorbates used as test molecules for TERS were the Brilliant Cresyl Blue laser dye (standard purity, Fluka) and sodium cyanide (p.a., Merck). Deposition from aqueous solutions (Millipore distilled water) at the metal electrodes was performed electrochemically for cyanide ions (NaCN 10^{-3} M, $NaClO_4$ 10^{-1} M used as supporting electrolyte) by polarizing at –750 mV *vs.* SCE; the electrode was emersed under potential control and any trace of the electrolyte on the surface blown away with a nitrogen flow.

A number of organic dyes easily form strong bonds with gold, among them BCB. In order to obtain a monolayer coverage at the surface, an extremely diluted solution of the dye (10^{-6} M) was used. A small device was assembled for deposition by wetting of the surface: the glass slide (10 mm by 20 mm) was fixed at a certain height with the gold film on the bottom side, a small teflon tube (diameter 5 mm) connected to a syringe containing the solution was positioned vertically below the film. A single droplet from the tube made contact with the gold film; the tube may be moved with respect to the film by a small motor drive, keeping always a meniscus between the tube and film. A dye coverage of about a monolayer has been estimated after the Raman experiments by redissolving the dye in methanol and measuring the resulting dye concentration in the solution by fluorescence intensity.

Other chemicals used for the surface preparation were: $HAuCl_4 \cdot 3H_20$ (p.a., Merck), $NaClO_4$ (p.a., Fluka), KCl (p.a., Fluka). Silver and gold wires (purity 99,998 %) were obtaind from Alfa Aesar.

3.6 Optics for STM-Emitted light detection

The set-up shown previously can be easily modified to enable the collection of light at a different angle with respect to the tip axis. In chapter two it was shown how direct information may be obtained about the resonant energies of the localized plasmon modes at the tip/sample junction. Briefly, these modes may be excited by inelastically tunneling electrons and then annihilated by generating light. Such a process has a relatively small probability and the overall sensitivity of the optics should be considered first.

For the experimentally determined quantum yield of photon emission by a tunneling electron, a value around 10^{-5} is given. It has also been shown that the emission of light is by no way isotropic but is a lobed function of the azimuthal angle peaking at 55° [88]. Thus, the objective used for the collection of light was mounted in such a way that its optical axis has an angle of 60° relative to the surface normal; its high numerical aperture ($n.a. = 0.55$, working distance 8 mm) ensures that a fraction of the emitted light equal to about 0.18 is collected.[5] The next point to be considered is that the energy of the emitted photons may be spread over a wide spectral range (from the near IR to the visible). The CCD camera (optimized for Raman measurements with the He-Ne laser) efficiently covers the frequency range of light emission between 650 nm and 1050 nm. This window is divided into 10^3 channels (pixels). A tunneling current of 20 nA gives a flow of electrons equal to $1.25 * 10^{11}\ e^- s^{-1}$. Gathering all these numbers we obtain for the number of photons to be expected per channel:

$$\underbrace{n}_{\text{recorded photons}} = \underbrace{1*10^{-5}}_{\text{quantum yield}} * \underbrace{1.25*10^{11}\frac{e^-}{s}}_{\substack{\text{number of}\\ \text{electrons tunneling}}} * \underbrace{0.18}_{\substack{\text{solid angle}\\ \text{of collection}}} * \underbrace{5*10^{-2}}_{\substack{\text{quantum efficiency}\\ \text{of the electron array}}} / \underbrace{10^3}_{\substack{\text{number}\\ \text{of channels}}} \simeq 10\frac{photons}{s*channels}.$$

[5] For a first, low bounded estimation, an isotropic emission over half a sphere is considered.

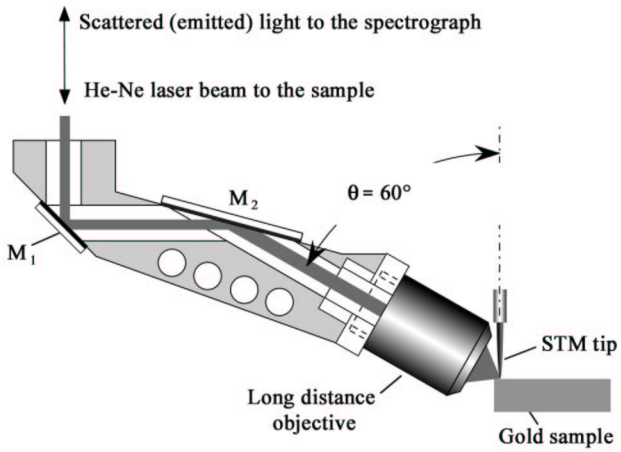

Figure 3.6: The 60° arrangement used for TERS and STM emitted light detection. The vertically incident light is directed by the two mirrors M_1 and M_2 into a direction that has an angle of 60° relative to the surface normal. The scattered light (or the emitted photons) collected by the objective is re-directed into the vertical path and then transfered to the spectrograph and CCD camera.

This value should be higher than the minimum signal to noise ratio. Actually, the intensity of the spectra recorded in air was much higher than expected (up to a few hundreds of counts per second) so that also smaller tunneling currents (and relatively short integration times) could be used.

This 60° arrangement has also been adopted for the TERS experiments, yielding a number of advantages. With the laser light incident on the sample from above, thicker films (or even single crystal electrodes) can be used and the heavy losses of the former approach, where the laser and scattered beams had to pass through the thin metal film, are absent.